Evolution of the equatorial oscillation in Saturn's stratosphere between 2005 and 2010 from Cassini/CIRS limb data analysis

Sandrine Guerlet, Thierry Fouchet, Bruno Bézard, Michael Flasar, Amy A. Simon-Miller

Evolution of the equatorial oscillation in Saturn's stratosphere between 2005 and 2010 from Cassini/CIRS limb data analysis

S. Guerlet,[1,2] T. Fouchet,[1,3,4] B. Bézard,[1] F. M. Flasar,[5] and A. A. Simon-Miller[5]

Received 18 February 2011; revised 28 March 2011; accepted 30 March 2011; published 4 May 2011.

[1] We present an analysis of thermal infrared spectra acquired in limb viewing geometry by Cassini/CIRS in February 2010. We retrieve vertical profiles of Saturn's stratospheric temperature from 20 hPa to 10^{-2} hPa, at 9 latitudes between 20°N and 20°S. Using the gradient thermal wind equation, we derive a map of the zonal wind field. Both the temperature and the zonal wind vertical profiles exhibit an oscillation in the equatorial region. These results are compared to the temperature and zonal wind maps obtained from 2005–2006 CIRS limb data, when this oscillation was first reported. In both epochs, strong temperature anomalies at the equator (up to 20K) are consistent with adiabatic heating (cooling) due to a sinking (rising) motion at a speed of 0.1–0.2 mm/s. Finally, we show that the altitude of the maximum eastward wind has moved downwards by 1.3 scale heights in 4.2 years, hence with a 'phase' speed of ~0.5 mm/s. This rate is consistent with the estimated period of 14.7 years for the equatorial oscillation, and requires a local zonal acceleration of 1.1×10^{-6} m.s^{-2} at the 2.5 hPa pressure level. This downward propagation of the oscillation is consistent with it being driven by absorption of upwardly propagating waves.
Citation: Guerlet, S., T. Fouchet, B. Bézard, F. M. Flasar, and A. A. Simon-Miller (2011), Evolution of the equatorial oscillation in Saturn's stratosphere between 2005 and 2010 from Cassini/CIRS limb data analysis, *Geophys. Res. Lett.*, *38*, L09201, doi:10.1029/2011GL047192.

1. Introduction

[2] Equatorial, cyclic oscillations are known to occur in the stratospheres of the Earth, Jupiter [*Simon-Miller et al.*, 2007] and Saturn. On Earth, the Quasi Biennal Oscillation (QBO) has been monitored and studied in detail since the 1950's (see *Baldwin et al.* [2001] for a review). It is characterized by alternate bands of eastward and westward winds that move downwards through the stratosphere. Thus, at a given pressure level, the zonal wind alternates between westward and eastward regimes, with an average period of 28 months. As the tropical temperatures are in thermal wind balance with the vertical shear of the zonal winds, the equatorial oscillations induce a strong thermal signature, where positive temperature anomalies are associated with eastward shear zones and negative anomalies with westward shear zones. The QBO is known to be triggered by interactions between the mean zonal flow and upward propagating waves, which transfer momentum to the atmosphere. The waves are damped in the shear zone below the jet maximum, locally accelarating the zonal wind, hence propagating the jet maximum downward, until it is viscously damped at the tropopause. When the jet disappears, the waves can freely propagate upward, triggering a new jet in the upper stratosphere that will again descend over time to close the cycle.

[3] On Saturn, a similar equatorial oscillation has been recently discovered using two different observational techniques. *Orton et al.* [2008] analyzed long-term infrared ground-based observations between 1989 and 2007. They reported cyclic variations of the relative brightness temperature between 3° and 15° of latitude, at one pressure level in the lower stratosphere (~20 hPa), with a period estimated to 14.7 ± 0.9 years. In the second study, *Fouchet et al.* [2008] measured pressure-latitude maps of the temperature from Cassini/CIRS limb data acquired in 2005 and 2006, establishing the vertical structure of the oscillation between 20 and 0.01 hPa. They also derived a map of the zonal wind, which displays an oscillation confined to the equator, with a strong vertical shear of 200 m/s between the location of the two extrema, located at 3 and 0.3 hPa at this time.

[4] Since then, *Fletcher et al.* [2010] reported strong temporal variation of the equatorial temperature at 1 hPa using CIRS nadir observations between 2005 and 2009. However, these studies have not adequately characterized how the structure of temperature and winds in the oscillation evolves with time. This missing information is essential to understand better the nature, properties and drivers of Saturn's equatorial oscillation. Here, we present an analysis of Cassini/CIRS limb data acquired in February 2010 in the equatorial region, allowing us to study the evolution of the 2-D thermal and zonal wind fields between 2005 and 2010.

2. Observations

[5] In order to measure the stratospheric temperature, we analyze spectra of Saturn's thermal emission acquired by CIRS, an infrared Fourier transform spectrometer onboard the Cassini spacecraft (see *Flasar et al.* [2004] for a complete description). In this study, we focus on CIRS data acquired in limb viewing geometry in the spectral range 600–1400 cm^{-1} (7–17 μm). The focal plane consists of two linear arrays of ten square detectors with an individual field of view (IFOV) of 0.273 × 0.273 mrad. In limb geometry, the two arrays are set perpendicular to the limb of the planet, so that each detector probes a different altitude. The pro-

[1]LESIA, Observatoire de Paris, Meudon, France.
[2]SRON Netherlands Institute for Space Research, Utrecht, Netherlands.
[3]Université Pierre et Marie Curie, UMR 8109, Paris, France.
[4]Institut Universitaire de France, Paris, France.
[5]NASA/Goddard Space Flight Center, Greenbelt, Maryland, USA.

0094-8276/11/2011GL047192

jected IFOV of one detector ranges from 50 to 100 km, thus 1 to 2 scale heights in the vertical direction and ~0.5° in latitude. This geometry allows us to measure vertical profiles of the temperature with both a very good vertical extent and spatial resolution.

[6] The limb data set analyzed in this study was acquired in February, 2010, at nine latitudes between 20°N and 20°S, every 5° of latitude, at the spectral resolution of 7.3 cm^{-1} (spectra are unapodized).

3. Retrieval Algorithm

[7] Our methodology is the following: assuming the mixing ratios of CH_4 and He, we retrieve temperature profiles from the analysis of the ν_4 emission band of methane (CH_4), centered at 1305 cm^{-1}, as well as the H_2-He collision-induced emission in the range 600–660 cm^{-1}. Spectra acquired by the different detectors, at different tangent altitudes, are treated simultaneously. A detailed description of our algorithm can be found in the work of *Guerlet et al.* [2009]; we only provide here a short description of its main elements.

3.1. Forward Model

[8] The forward model, **F**, consists of a line-by-line radiative transfer model adapted to spherical geometry. Our atmospheric model comprises 360 layers equally spaced in terms of Log(pressure), at pressure levels ranging from 10^6 to 10^{-3} Pa. The state vector **x** comprises the temperature profile and an altitude shift to account for uncertainties in the tangent altitudes given by navigation (typically a few tens of kilometers). Auxiliary parameters are the vertical profile of CH_4 (taken from *Moses et al.* [2000], with a homopause level at 0.1 μbar), the mixing ratios of H_2 and He (respectively set to 0.86 and 0.1355, as obtained by *Conrath and Gautier* [2000]), and spectroscopic data.

3.2. Retrieval Technique

[9] The considered inverse problem is an ill-posed and under-constrained problem. To solve it, we use the optimal estimation theory [*Rodgers*, 2000], which consists of finding an optimal solution $\hat{x}$ by minimizing a cost function, Q, that includes our *a priori* knowledge on the state vector:

$$Q = (\mathbf{y} - \mathbf{F}(\mathbf{x}))^T \mathbf{S}_e^{-1} (\mathbf{y} - \mathbf{F}(\mathbf{x})) + (\mathbf{x} - \mathbf{x}_a)^T \mathbf{S}_a^{-1} (\mathbf{x} - \mathbf{x}_a) \quad (1)$$

where **y** is the measured radiance, S_e is the measurement error covariance matrix, $\mathbf{x}_a$ the *a priori* state vector and $\mathbf{S}_a$ the *a priori* covariance matrix. The solution (temperature profile and vertical shift) is obtained through an iterative process that follows the constrained linear inversion method detailed by *Conrath et al.* [1998]. The sensitivity of the measurement to the temperature is given by the matrix **K** defined by $K_{ij} = \frac{\partial y_i}{\partial x_j}$, where index i refers to a wavenumber ν_i and index j to a pressure level p_j. The study of these functional derivatives shows that CH_4 emission band is sensitive to stratospheric temperatures from ~2 hPa to 10^{-2} hPa, whereas the H_2-He continuum provides information in the region 20–0.5 hPa.

[10] This retrieval method has been tested on synthetic retrievals and yields satisfactory results (see *Guerlet et al.* [2009] for examples). The error budget, comprising the propagation of the noise, a smoothing error and the propagation of the error on the auxiliary parameters (except spectroscopic data), yields errors of 1 K to 1.5 K in the pressure range 20–0.01 hPa.

4. Results

4.1. Temperature Map

[11] We present in Figure 1 (middle) the temperature map we obtain by combining the 2010 temperature profiles retrieved at latitudes between 20°N and 20°S. We also show, for comparison, the map we previously obtained from limb data acquired between March, 2005 and February, 2006 [see *Fouchet et al.*, 2008; *Guerlet et al.*, 2009], as well as the difference between the two maps (Figure 1, right). The same observational designs, forward model and retrieval technique were used for the two limb data sets.

[12] We note that in 2010, the equatorial oscillation is still present in the thermal structure of Saturn's stratosphere, although the alternating pattern of cold and warm anomalies at the equator has changed. For instance, the cold anomaly observed at the equator at 0.1 hPa in 2005/2006 is now located at 0.3 hPa. At a given epoch, these temperature anomalies are the signatures of a meridional circulation, with warming of the stratosphere associated to subsidence and adiabatic cooling due to upwelling. Such circulation cells are observed on Earth, associated to the QBO, and contributes to maintaining the geostrophic balance [*Baldwin et al.*, 2001]. We can estimate the windspeed of these vertical motions at the equator with the use of a *static* heat balance [*Andrews*, 2000]:

$$\frac{N^2 H w}{R/M} = J \quad \text{with} \quad N^2 = \frac{R}{H}\left(\frac{dT}{dz} + \frac{RT}{C_p H}\right) \quad (2)$$

where N is the Brunt-Väisäla frequency, H is the vertical scale height, R is the gas constant, M the mean molar mass, T the temperature and C_p the specific heat. Here, the vertical motion term balances a radiative relaxation term J that can be parameterized with a radiative time constant τ_{rad}, as $J = \frac{\Delta T}{\tau_{rad}}$. From the study of *Conrath et al.* [1990], τ_{rad} can be estimated to 3×10^{-8} s at 1 hPa. Given that at this pressure level and in the equatorial region, H equals 55 km and N^2 equals 5×10^{-5} s^{-2}, a temperature anomaly of 20 K with respect to the surrounding latitudes corresponds to a vertical wind speed of 0.1 mm/s. This value is of the same order of magnitude than an earlier estimate obtained by *Guerlet et al.* [2009]. Mapping the C_2H_2 and C_2H_6 meridional profiles from the Cassini/CIRS observations, these authors found an enhancement of the abundance in the two gases at the equator that could be explained by the descent of hydrocarbon-rich air, with a vertical wind speed at the equator of 0.2 ± 0.1 mm/s at 1 hPa. Hence, both the temperature and the chemical equatorial anomalies observed by CIRS are consistent with subsidence of ~0.1–0.2 mm/s.

[13] We also report temporal changes in temperature that are well above our error bars. For instance, at the 0.5 hPa level, the stratosphere has warmed up by 10 to 20 K in the regions located at 15–20° North and South of the equator, whereas it has cooled down by more than 20 K at the equator. Furthermore, equatorial temperatures have risen by ~10 K around 5 and 0.01 hPa. These temporal changes cannot be caused by the seasonal variations of insolation, as this kind of heating or cooling should be rather

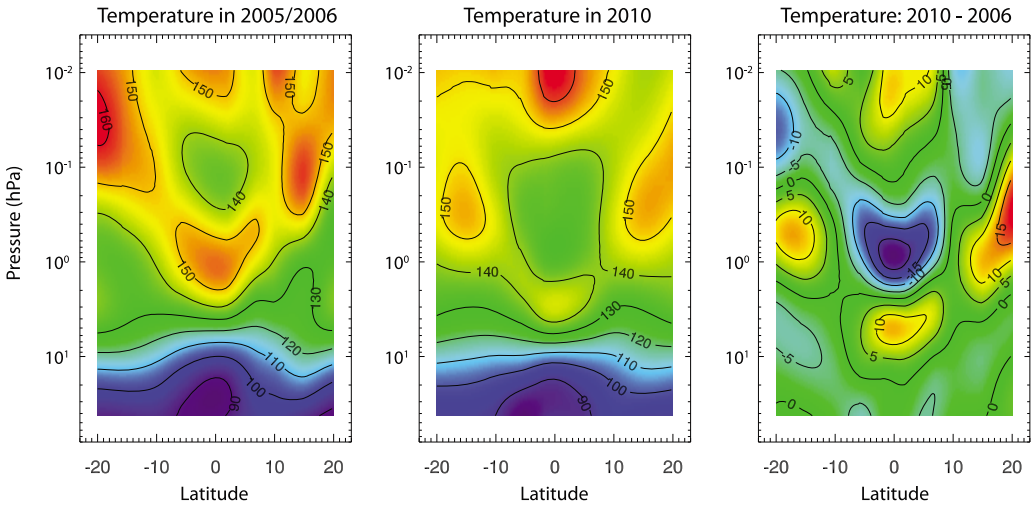

Figure 1. (left to right) Temperature maps (in Kelvin) obtained from Cassini/CIRS limb data acquired in 2005–2006 [*Fouchet et al.*, 2008], in 2010 (this study) and the difference of temperature between the two dates.

homogeneous with altitude, or at least of the same sign. In addition, the amplitudes of the changes are too large to be consistent with a seasonal radiative forcing. For example, using a seasonal radiative model, *Fletcher et al.* [2010] predicted a temperature change of only ~2 K at the equator at 1 hPa between 2004 and 2009. These strong temporal changes are rather the signature of the downward propagation of the oscillation (see section 4.2).

4.2. Zonal Wind Map

[14] The zonal wind u is retrieved integrating in cylindrical coordinates the modified thermal wind equation [*Flasar et al.*, 2005]:

$$\frac{\mathrm{d}}{\mathrm{d}z_{\|}}\left(\frac{u^2}{r\cos\theta_{PC}}+2\Omega u\right)=-\frac{g}{Tr}\left(\frac{\partial T}{\partial\theta_{PG}}\right)_p \qquad (3)$$

with θ_{PC} and θ_{PG} the planetocentric and planetographic latitudes, Ω the Saturn angular velocity, r the local radius, $z_{\|}$ the distance from the equatorial plane along the axis of rotation, p the pressure, and g the gravity.

[15] Since in limb viewing geometry we are unable to probe the temperature field from the stratosphere down to the cloud top, where the winds are measured by cloud tracking, the equation was integrated along cylinders parallel to the axis of rotation from the 20-hPa pressure level, where the zonal wind is set to zero. The calculated winds are thus relative to that at the 20-hPa level, and not absolute values.

[16] The thermal winds maps obtained using the 2005–2006 and 2010 thermal maps are compared in Figure 2 (top). The comparison reveals that the overall structure of alternating eastward and westward jets has moved downwards. This temporal evolution is qualitatively similar to the evolution of the QBO on Earth. The strong eastward jet located at 0.3 hPa in 2006 is, in 2010, centered around 1.1 hPa. It has hence descended by 1.3 scale height in 4.2 years. This value corresponds to a downward 'phase' speed of w_{phase} ~ 0.5 mm/s for the oscillation pattern. Since the two jets are separated by 2.3 scale heights, a complete cycle would take approximately 14.9 years. This estimate, based on the monitoring of the vertical structure of Saturn's equatorial oscillation, is in excellent agreement with the period of 14.7 ± 0.9 years infered by *Orton et al.* [2008] from long term monitoring of the temperature structure at a single pressure level (20 hPa). The strong westward jet located at 5 hPa in 2006 has similarly moved downwards in 2010, but its amplitude has also greatly diminished. This amplitude decay could be due to a mechanical damping by eddy viscosity as the jet approaches the tropopause level. However, we cannot rule out that this apparent decrease in amplitude is an artifact of our inversion method. At 10 hPa, as we approach the bottom limit of the altitude range probed by our observations, the inverted temperature profiles relax towards the *a priori* profile, underestimating the meridional thermal contrasts, hence the zonal winds. The analysis by *Schinder et al.* [2011] of Cassini radio occultation profiles tends to support this latter hypothesis, as they retrieved warmer equatorial temperatures at 5–10 hPa than we do.

[17] Using a wave analogy, changes in the temperature field are proportional to the thermal vertical gradient and the descent rate of the pattern, as expressed by the equation: $\frac{\partial T}{\partial t}=-w_{phase}\frac{\partial T}{\partial z}$. Given that the average lapse rate between adjacent cold and warm regions vertically stacked to be ~20 K per 2 scale heights and using the previous estimate of w_{phase}, we find $\frac{\partial T}{\partial t}$ ~ 13 K in 4.2 years. This is the right order of magnitude for the temporal changes observed (see Figure 1, right).

[18] Figure 2 (bottom) displays the difference between the thermal winds maps obtained in 2005–2006 and 2010, hence the local acceleration of the zonal wind. Two alternate bands of zonal acceleration appear very clearly: an eastward acceleration band centered at 2.5 hPa and a westward acceleration band centered at 0.15 hPa. The maximum eastward acceleration reaches 1.1×10^{-6} m.s^{-2}, while the peak westward acceleration reaches 1.4×10^{-6} m.s^{-2}. The fact that the maximum acceleration occurs just below the core of the jet strongly suggests that, as on Earth, the oscillation is driven by upward propagating waves, damped and depositing their momentum just beneath the core of

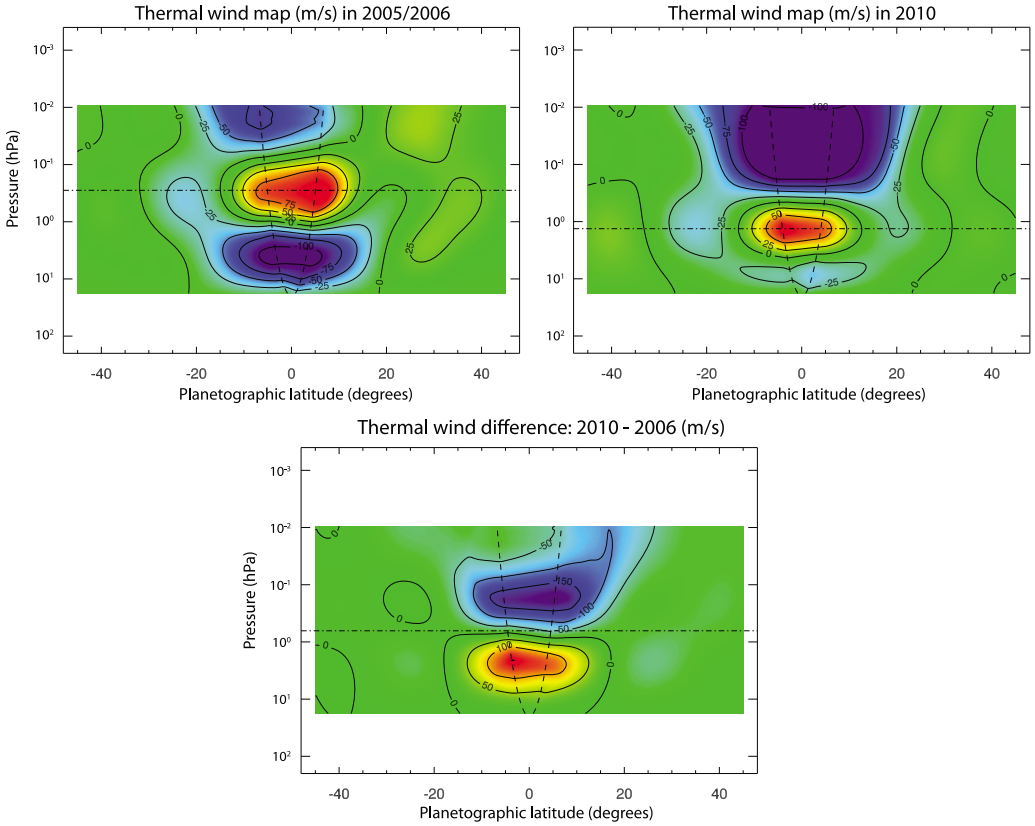

Figure 2. Map of the thermal zonal wind obtained from Cassini/CIRS limb data acquired in (top left) 2005–2006 [*Fouchet et al.*, 2008]), (top right) 2010 (this study), and (bottom) the difference between the two maps. The horizontal dot-dashed lines on the three panels highlight the altitude of the eastward jet respectively in 2005–2006, 2010, and the average altitude between the two dates. Equatorward and above the line defining the cylinder tangent to the equator at 20 hPa, the wind field is unconstrained by the thermal wind equation, and it has been linearly interpolated on constant pressure surfaces. The error on u given the uncertainties on T is about 5 m.s^{-1}.

the jet. For Jupiter, *Li and Read* [2000] used an analytical and a numerical model to investigate the upward propagation of waves in the jovian upper troposphere and stratosphere. They calculated the divergence of the Eliassen-Palm flux resulting from the interaction of these waves with the mean zonal flow, and found that it could account for a few 10^{-6} m.s^{-2} of zonal wind acceleration, in agreement with the observed QQO amplitude. As Jupiter and Saturn bear many similarities in terms of dynamical, thermal, and chemical structures, we view the quantitative agreement between the jovian QQO model and the observed kronian oscillation as an additional clue for the driving role of equatorial waves in Saturn's equatorial oscillation.

5. Conclusion and Perspectives

[19] This study reveals for the first time the temporal evolution of the thermal and zonal wind fields (with latitude and altitude) of Saturn's equatorial oscillation. It shows that the main features of the oscillation, local extrema of temperature and jets, have moved downwards with time, consistently with a close to 15 years period (half a kronian year). The 'phase' speed of the oscillation pattern is ~0.5 mm/s, whereas evidence for subsidence and upwelling are seen through temperature anomalies at a given epoch, with vertical speed motions estimated in the range 0.1–0.2 mm/s. This behavior is extremely reminiscent of the terrestrial QBO and strongly advocates for the similarity of the terrestrial, jovian, and kronian phenomena. However, in contrast with its terrestrial and jovian counterparts, the kronian equatorial oscillation has a period which is commensurate with the saturnian year. Numerical studies will have to state whether this proportionality is fortuitous or whether it arises from Saturn's specificities, such as the ring's shadow which enforces strong seasonal signal in the tropics.

[20] On Earth, the QBO is forced from both eastward and westward waves, with zonal phase velocities of comparable magnitude. On Saturn, only westward waves have been observed in the equatorial stratospheric temperature field by *Liming et al.* [2008], and their vertical structure has not been measured. The potential importance of the influence of equatorial waves on the tropical dynamics of Saturn's stratosphere requires that the nature, amplitude and spectrum of these waves should be much better characterized than they are currently. At a small vertical scale (typically a tenth of a scale height), radio occultation measurements seem the most powerful means to constrain the wave amplitude and spectrum. At a larger vertical scale (1–2 scale heights), CIRS limb observations spanning at least 120°–180° of longitude would be needed to simultaneously observe the zonal and vertical structure of equatorial waves. Such observations should be conducted in the course of the Cassini Solstice Mission.

[21] **Acknowledgments.** We thank the Cassini/CIRS team for putting a lot of efforts in the planning and calibration of the data. This work is partly supported by the Programme National de Planétologie (PNP/INSU) and by the Centre National d'Etudes Spatiales (CNES). We also thank the two anonymous referees for their useful comments.

[22] The Editor thanks two anonymous reviewers for their assistance in evaluating this paper.

References

Andrews, D. (2000), *An Introduction to Atmospheric Physics*, Cambridge Univ. Press, Cambridge, U. K.

Baldwin, M. P., et al. (2001), The quasi-biennial oscillation, *Rev. Geophys.*, *39*, 179–230.

Conrath, B. J., and D. Gautier (2000), Saturn helium abundance: A reanalysis of Voyager measurements, *Icarus*, *144*, 124–134, doi:10.1006/icar.1999.6265.

Conrath, B. J., P. J. Gierasch, and S. S. Leroy (1990), Temperature and circulation in the stratosphere of the outer planets, *Icarus*, *135*, 255–281, doi:10.1016/0019-1035(90)90068-K.

Conrath, B. J., P. J. Gierasch, and E. A. Ustinov (1998), Thermal structure and para hydrogen fraction on the outer planets from Voyager IRIS measurements, *Icarus*, *135*, 501–517, doi:10.1006/icar.1998.6000.

Flasar, F. M., et al. (2004), Exploring the Saturn system in the thermal infrared: The composite infrared spectrometer, *Space Sci. Rev.*, *115*, 169–297, doi:10.1007/s11214-004-1454-9.

Flasar, F. M., et al. (2005), Titan's atmospheric temperatures, winds, and composition, *Science*, *308*, 975–978, doi:10.1126/science.1111150.

Fletcher, L. N., R. K. Achterberg, T. K. Greathouse, G. S. Orton, B. J. Conrath, A. A. Simon-Miller, N. Teanby, S. Guerlet, P. G. J. Irwin, and F. M. Flasar (2010), Seasonal change on Saturn from Cassini/CIRS observations, 2004–2009, *Icarus*, *208*, 337–352, doi:10.1016/j.icarus.2010.01.022.

Fouchet, T., S. Guerlet, D. F. Strobel, A. A. Simon-Miller, B. Bézard, and F. M. Flasar (2008), An equatorial oscillation in Saturn's middle atmosphere, *Nature*, *453*, 200–202, doi:10.1038/nature06912.

Guerlet, S., T. Fouchet, B. Bézard, A. A. Simon-Miller, and F. M. Michael Flasar (2009), Vertical and meridional distribution of ethane, acetylene and propane in Saturn's stratosphere from CIRS/Cassini limb observations, *Icarus*, *203*, 214–232, doi:10.1016/j.icarus.2009.04.002.

Li, X., and P. L. Read (2000), A mechanistic model of the quasi-quadrennial oscillation in Jupiter's stratosphere, *Planet. Space Sci.*, *48*, 637–669, doi:10.1016/S0032-0633(00)00033-7.

Liming, L., P. J. Gierasch, R. K. Achterberg, B. J. Conrath, F. M. Flasar, A. R. Vasavada, A. P. Ingersoll, D. Banfield, A. A. Simon-Miller, and L. N. Fletcher (2008), Strong jet and a new thermal wave in Saturn's equatorial stratosphere, *Geophys. Res. Lett.*, *35*, L23208, doi:10.1029/2008GL035515.

Moses, J. I., B. Bézard, E. Lellouch, G. R. Gladstone, H. Feuchtgruber, and M. Allen (2000), Photochemistry of Saturn's atmosphere. I. Hydrocarbon chemistry and comparisons with ISO observations, *Icarus*, *143*, 244–298, doi:10.1006/icar.1999.6270.

Orton, G. S., et al. (2008), Semi-annual oscillations in Saturn's low-latitude stratospheric temperatures, *Nature*, *453*, 196–199, doi:10.1038/nature06897.

Rodgers, C. D. (2000), *Inverse Methods for Atmospheric Sounding*, World Sci., Singapore.

Schinder, P. J., F. M. Flasar, E. A. Marouf, R. G. French, C. A. McGhee, A. J. Kliore, N. J. Rappaport, E. Barbinis, D. Fleischman, and A. Anabtawi (2011), Saturn's equatorial oscillation: Evidence of descending thermal structure from Cassini radio occultations, *Geophys. Res. Lett.*, doi:10.1029/2011GL047191, in press.

Simon-Miller, A. A., B. W. Poston, G. S. Orton, and B. Fisher (2007), Wind variations in Jupiter's equatorial atmosphere: A QQO counterpart?, *Icarus*, *186*, 192–203, doi:10.1016/j.icarus.2006.08.009.

B. Bézard, T. Fouchet, and S. Guerlet, LESIA, Observatoire de Paris, 5 Place Jules Janssen, F-92195 Meudon, France. (sandrine.guerlet@obspm.fr)

F. M. Flasar and A. A. Simon-Miller, NASA/Goddard Space Flight Center, Code 693,Greenbelt, MD 20771, USA.